Proton Release and Uptake of *pharaonis* Phoborhodopsin (Sensory Rhodopsin II) Reconstituted into Phospholipids†

Masayuki Iwamoto,*,‡,§ Chisa Hasegawa,§ Yuki Sudo,§ Kazumi Shimono,§ Tsunehisa Araiso,‡ and Naoki Kamo§

Laboratory of Biomolecular Systems, Center for Advanced Science and Technology, Hokkaido University, Sapporo 001-0021, Japan, and Laboratory of Biophysical Chemistry, Graduate School of Pharmaceutical Sciences, Hokkaido University, Sapporo 060-0812, Japan

Received November 4, 2003; Revised Manuscript Received January 22, 2004

ABSTRACT: *pharaonis* phoborhodopsin (*p*pR, also called *pharaonis* sensory rhodopsin II, *p*sRII) is a photoreceptor for negative phototaxis in *Natronobacterium pharaonis*. During the photoreaction cycle (photocycle), *p*pR exhibits intraprotein proton movements, resulting in proton pumping from the cytoplasmic to the extracellular side, although it is weak. In this study, light-induced proton uptake and release of *p*pR reconstituted with phospholipid were analyzed using a SnO_2 electrode. The reconstituted *p*pR exhibited properties in proton uptake and release that are different from those of dodecyl maltoside solubilized samples. It showed fast proton release before the decay of ppR_M (M-photointermediate) followed by proton uptake, which was similar to that of bacteriorhodopsin (BR), a light-driven proton pump. Mutant analysis assigned Asp193 to one (major) of the members of the proton-releasing group (PRG). Fast proton release was observed only when the pH was approximately 5−8 in the presence of Cl^-. When Cl^- was replaced with SO_4^{2-}, the reconstituted *p*pR did not exhibit fast proton release at any pH, suggesting Cl^- binding around PRG. PRG in BR consists of Glu204 (Asp193 in *p*pR) and Glu194 (Pro183 in *p*pR). Replacement of Pro183 by Glu/Asp, a negatively charged residue, led to Cl^--independent fast proton release. The transducer binding affected the properties of PRG in *p*pR in the ground state and in the ppR_M state, suggesting that interaction with the transducer extends to the extracellular surface of *p*pR. Differences and similarities in the molecular mechanism of the proton movement between *p*pR and BR are discussed.

pharaonis phoborhodopsin (*p*pR,[1] also called *pharaonis* sensory rhodopsin II, *p*sRII) (*1*−*6*) is a member of an archaeal rhodopsin family and acts as a negative phototaxis receptor in *Natronomonas* (*Natronobacterium*) *pharaonis*. Phototaxis is achieved by modulating cell swimming behavior through light-activated signal transduction from *p*pR to a cognate transducer protein, *pharaonis* halobacterial transducer II (*p*HtrII). *p*pR has seven transmembrane helices into which a chromophore, all-*trans*-retinal, binds through a protonated Schiff base (see Figure 1). This feature is common among other archaeal rhodopsins such as bacteriorhodopsin (BR) (*7*−*9*), halorhodopsin (HR) (*10*−*12*), and sensory rhodopsin (sR or sRI) (*13*, *14*), which are an outwardly light-driven proton pump, an inwardly light-driven Cl^- pump, and another sensor of phototaxis, respectively. Thousands of

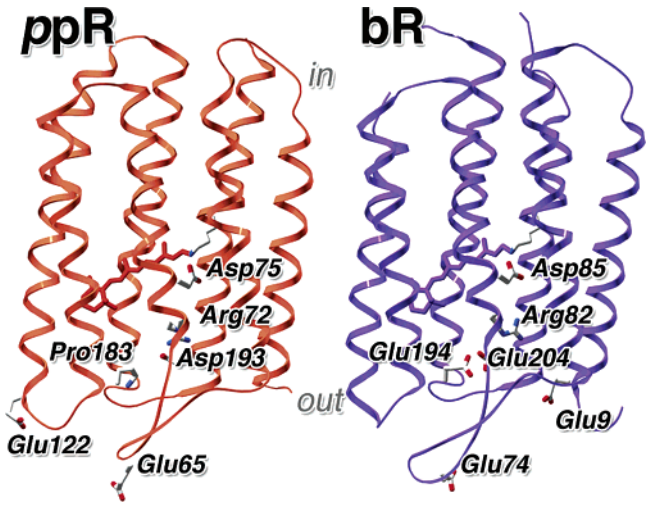

FIGURE 1: X-ray crystallographic structures of *p*pR and BR. The retinal chromophore which is bound to Lys205 (*p*pR) or Lys216 (BR) on helix G through the Schiff base, important residues for proton transfer in the extracellular channel, and carboxylic acid residues in the extracellular surface are depicted as bold abbreviations and sticks in the ribbon drawing of the backbone structures. These structures were taken from the Protein Data Bank (PDB), codes 1H68 for *p*pR and 1C3W for BR.

† This work was supported by research fellowships from the Japan Society for the Promotion of Science for Young Scientists to M.I.

* To whom correspondence should be addressed. Phone: +81-11-706-3923. Fax: +81-11-706-4984. E-mail: iwamoto@cast.hokudai.ac.jp.

‡ Laboratory of Biomolecular Systems, Center for Advanced Science and Technology, Hokkaido University.

§ Laboratory of Biophysical Chemistry, Graduate School of Pharmaceutical Sciences, Hokkaido University.

[1] Abbreviations: *p*pR, *pharaonis* phoborhodopsin; *p*HtrII, *pharaonis* halobacterial transducer II; $pHtrII_{1-159}$, *pharaonis* halobacterial transducer II expressed from position 1 to position 159; ppR_K, K-intermediate of *p*pR; ppR_M, M-intermediate of *p*pR; ppR_O, O-intermediate of *p*pR; BR, light-adapted bacteriorhodopsin; BR_M, M-intermediate of BR; DM, *n*-dodecyl *β*-D-maltoside; PC, L-α-phosphatidylcholine from egg; Caps, 3-(cyclohexylamino)-1-propanesulfonic acid; Ches, 2-(*N*-cyclohexylamino)ethanesulfonic acid; Hepes, *N*-(2-hydroxyethyl)piperazine-*N*′-2-ethanesulfonic acid; Mes, 2-(*N*-morpholino)ethanesulfonic acid; Mops, morpholinopropanesulfonic acid.

10.1021/bi035960n CCC: $27.50
Published on Web 02/26/2004

investigations concerning the structure and function of BR have been reported, and consequently, BR is one of the best understood membrane proteins. However, the other archaeal rhodopsins are less understood than BR.

The functional expression of *p*pR in *Escherichia coli* cells (*15*) has been achieved, which affords a large amount of proteins to be characterized in detail. The crystal structures of *p*pR were solved by two groups (*16*, *17*) and show almost the same 3D structure between *p*pR and BR (Figure 1). This fact implies that functional differentiation of these two proteins originates from slight differences in amino acid side chains. Furthermore, the crystal structure of the *p*pR−*p*HtrII complex (*18*) has been reported. The solution to these X-ray structures opened the next stage of research on this photosensor.

The photocycle intermediates in *p*pR are denoted K, L, M, N, and O in analogy to those for BR. The presence of the N-intermediate was suggested by multiexponential global analysis of the photocycle of *p*pR (*3*), whereas its nature is not well understood. In fact, FTIR studies (*19*, *20*) revealed that *p*pR does not possess the N-like protein structure that is characteristic of the N-intermediate of BR. Upon BR_M formation during the BR photocycle, primary proton transfer from the protonated Schiff base to its counterion, Asp85, and subsequent proton release from the proton-releasing group (PRG) to the extracellular side occur. The following cascade of proton movements such as uptake from the intracellular side and the transfer from Asp96 to the deprotonated Schiff base at the end of the photocycle results in proton pumping of BR from the cytoplasmic to the extracellular side. *p*pR also exhibits proton transfer from the protonated Schiff base to its counterion, Asp75, upon pR_M formation (*19*, *21*) like BR and can pump protons from the cytoplasmic to the extracellular side although its activity is weak (*22*, *23*). The proton pumping activity of *p*pR is ceased by association with its transducer, *p*HtrII (*23*, *24*), while proton circulation (futile proton uptake and release for pumping) during the photocycle is still observed (*23*). Proton uptake and release during the photocycle of dodecyl maltoside (DM) solubilized *p*pR were previously analyzed in detail by using a SnO_2 transparent electrode (*25*). In the solubilized state, *p*pR takes up a proton upon pR_O formation and releases it upon pR_O decay. The timing of proton uptake and release in *p*pR is different from that in BR; proton release occurs first upon BR_M formation, followed by the uptake upon BR_M decay. These differences are interesting because one of the residues corresponding to PRG in BR (Glu194) is not conserved in *p*pR (Pro183) (*26*). Detailed analysis of differences in the timing of proton uptake and release should be a focus for understanding the molecular mechanism of functional differentiation between these two archaeal rhodopsins.

In this study, we analyzed proton uptake and release during the photocycle of *p*pR reconstituted with phospholipids. Reconstituted *p*pR exhibits properties during proton uptake and release that are different from those of the DM-solubilized sample. Reconstituted *p*pR exhibits fast proton release under pHs between 5 and 8 in the presence of Cl^-: it releases proton before pR_M decay (in the time range of 100 ms), followed by slower proton uptake (continued until ~s). It is worthwhile to note that, in the absence of Cl^-, reconstituted *p*pR do not exhibit fast proton release at any pH. This suggests that Cl^- binding around the extracellular surface or PRG in *p*pR is indispensable for fast proton release. The critical component of PRG in *p*pR is proposed to be Asp193, which corresponds to Glu204 in BR (Figure 1). The PRG in BR consists of Glu204 and Glu194. Replacement of Pro183 in *p*pR (corresponding to Glu194 in BR) by a negatively charged residue, Glu/Asp, leads to Cl^--independent fast proton release: a mutant having Asp193 and a negative charge at position 183 shows more BR-like light-induced proton uptake and release than the wild type. Moreover, the pK_a shift of PRG from the *p*pR ground state to the pR_M state becomes close to that of BR by this replacement. In other words, BR-like PRG in *p*pR is partially formed by the mutation of Pro to Glu/Asp at position 183. Transducer binding also affects the properties of PRG in *p*pR in the ground state and in the pR_M state, suggesting that the effect of interaction with *p*HtrII extends to the extracellular surface by some means or contact also occurs at this place. The differences and similarities in the molecular mechanisms of proton transfer reactions between *p*pR and BR are discussed.

MATERIALS AND METHODS

Preparation of ppR and pHtrII Samples. The expression and purification of histidine-tagged recombinant *p*pR, its mutant proteins and $pHtrII_{1-159}$ were performed as previously described (*27*, *28*). Here, $pHtrII_{1-159}$ represents *pharaonis* halobacterial transducer II expressed from position 1 to position 159. Briefly, *p*pR and $pHtrII_{1-159}$ proteins possessing a histidine tag at the C-terminus were expressed in *E. coli* cells, solubilized with 1.5% *n*-dodecyl β-D-maltoside (DM), and purified by a Ni column. The purified sample was then mixed with L-α-phosphatidylcholine (PC) in the presence of Bio-Beads (Bio-Rad, Hercules, CA) where the molar ratio of added PC was 50 times that of *p*pR. Because of the small molar ratio of PC to *p*pR (approximately 50), this *p*pR sample reconstituted with PC did not form a closed vesicle but remained a membrane sheet. Actually, no entrapping of [^{3}H]-glucose was observed (data not shown). To prepare the *p*pR−*p*HtrII complex, purified *p*pR and $pHtrII_{1-159}$ proteins were mixed with a molar ratio ($pHtrII_{1-159}$/*p*pR) of 0, 0.5, 1, 2, or 3 and incubated for 1 h at 4 °C. The molar ratio of added PC/*p*pR was the same as that for the reconstitution of *p*pR alone as described above. The mixture was then reconstituted with PC using Bio-Beads, where the molar ratio of added PC was 50 times that of *p*pR.

Measurement of Light-Induced Proton Uptake and Release of PC-Reconstituted ppR. The PC-reconstituted samples were washed three times and suspended in distilled water. Then 50−100 μL of this suspension (approximately10 μM *p*pR) was dropped on a transparent SnO_2 electrode surface and dried with a diameter of 10 mm. The adhesion was so strong that the protein did not detach from the electrode surface unless washed with detergent. This conclusion was reached because repeated use was possible without any change in the signal amplitude. The SnO_2 electrode was used as a working electrode, and another SnO_2 electrode was used as a counter electrode. The solution in the electrochemical cell was 400 mM NaCl or 133 mM Na_2SO_4 supplemented with a mixture of six buffers (containing citric acid, Mes, Hepes, Mops, Ches, and Caps, all at 1 mM each) whose pH was adjusted with H_2SO_4 or NaOH to desired values. Note that

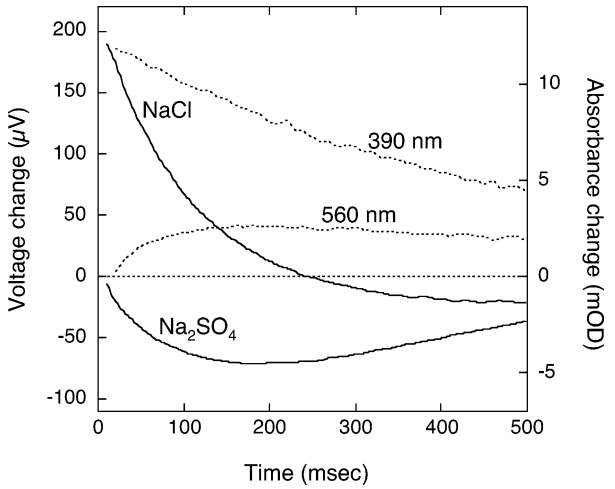

FIGURE 2: Light-induced pH and absorbance changes derived from PC-reconstituted *p*pR. The solid lines represent the light-induced pH change in the presence of NaCl or Na_2SO_4 at pH 5. The positive change is due to acidification of the SnO_2 electrode surface, and the negative is due to alkalization. The electrolyte solution contained 400 mM NaCl or 133 mM Na_2SO_4. The ionic strengths of these solutions were equal to each other. The broken lines represent the light-induced absorbance change at 390 or 560 nm in the presence of 400 mM NaCl at pH 5. The absorbance change at 390 and 560 nm was used to monitor the concentration change of ppR$_M$ and ppR$_O$, respectively. Almost the same absorption traces were obtained in the presence of 133 mM Na_2SO_4 at pH 5 (data not shown).

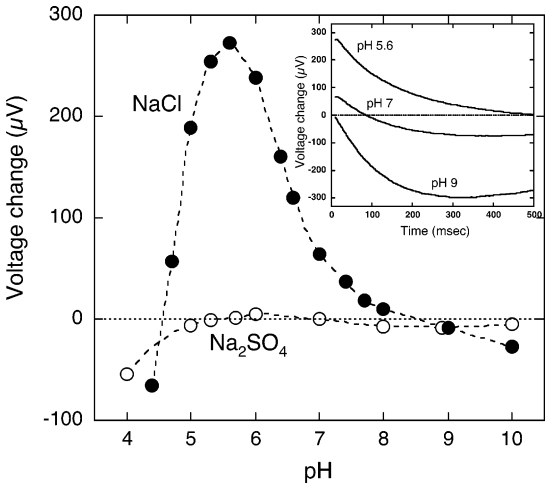

FIGURE 3: pH change of the electrode surface 10 ms after the photoexcitation of PC-reconstituted *p*pR under varying pHs. The value represents the pH change upon *p*pR-to-*p*pR$_M$ transition. The positive values stand for fast proton release before *p*pR$_M$ decay while the negative values stand for proton uptake, which means a delay of proton release that probably occurs during *p*pR$_O$ decay. The closed circles represent the data in the presence of 400 mM NaCl; the open circles, 133 mM Na_2SO_4. Inset: Typical data of the time course of light-induced pH changes. The data at pH 5.6, 7, and 9 were depicted. The electrolyte solution contained 400 mM NaCl.

the mixed buffer had a constant buffer strength in the pH range used. The electric circuit used and the generation of pulse light were the same as previously described (*20*, *25*). The low-cut frequency of the amplifier was set at 0.08 Hz. In this mode, the very slow baseline deflection (in the dark) was eliminated, and actinic light-elicited responses that were faster than a range of 12.5 s were amplified. The time range we were concerned with in this experiment was less than 0.5 s. Using a flash-light as an actinic light enabled the estimation of the timing of proton movement during photocycling (compare data in refs *25* and *20*). The presence of a high buffer solution in the electrochemical cell (e.g., 100 mM instead of 1 mM) eliminated flash-induced responses, implying that the origin of electric signals in the cell was the pH change on the working SnO_2 electrode surface. Therefore, the signals obtained were equal to the pH change at the surface of the working electrode as confirmed by a previous study (*25*).

Flash Photolysis Spectroscopy. The apparatus and the procedure for flash photolysis spectroscopy were essentially the same as previously described (*29*).

RESULTS

Proton Uptake and Release at pH 5 during the Photocycle of Wild-Type ppR Reconstituted with Phosphatidylcholine (PC). The time course of light-induced electric signals from the SnO_2 electrode, on which PC-reconstituted wild-type *p*pR was adhered to, was measured in the presence or absence of Cl^- at pH 5 (Figure 2, solid lines). A positive change was due to a decrease in local pH on the electrode surface (i.e., the proton release from *p*pR), and a negative change was caused by proton uptake. When Na_2SO_4 was used as an electrolyte (Cl^--free condition keeping ionic strength), the electric signal observed after the photoexcitation of *p*pR had a negative sign, indicating the proton uptake preceded proton release during the photocycle. The flash photolysis data of the wild-type *p*pR are depicted as broken lines in Figure 2. Time-dependent absorbance changes at 390 and 560 nm show the concentration change of *p*pR$_M$ and *p*pR$_O$ during the photocycle, respectively. Under the Cl^--free condition, the pH change after photoexcitation was proportional to that of *p*pR$_O$ (i.e., proton uptake and release coincided with the formation and decay of *p*pR$_O$, respectively). This result is the same as in our previous work (*25*), where DM-solubilized *p*pR was used. On the contrary, a light-induced fast positive signal (acidification of the electrode surface immediately after the flash) was observed when NaCl was used as an electrolyte while the fast acidification signal was not observed in Na_2SO_4 solution (Figure 2). The fast positive signal arose within less than several milliseconds. We were certain that the rise of the positive signal (proton release) occurred before *p*pR$_M$ decay, although the time resolution of our measuring system was not precise enough to detect the rise of this positive signal. It is noted that the *p*pR$_M$ decay rate is slow ($t_{1/2}$, ~300 ms at pH 5) compared with that for BR$_M$ ($t_{1/2}$, ~5 ms). Decay of the positive signal was somewhat faster than *p*pR$_M$ decay (absorbance change at 390 nm). Proton release before *p*pR$_M$ decay was not detected for DM-solubilized *p*pR even in the presence of Cl^- (*25*). Our present results suggest that a proton-releasing group (PRG) in *p*pR is affected by the environment: it is exposed to (in micelles or in the membrane) and specific anions such as Cl^-.

Identification and Characterization of PRG of PC-Reconstituted ppR. In BR, four Glu residues are located close to the extracellular surface, Glu9, Glu74, Glu194, and Glu204 (Figure 1). Two of them, Glu194 and Glu204, are part of the PRG (*30*−*32*), from which protons are released to the extracellular side upon BR$_M$ formation. On the other hand, three carboxylic residues, Glu65, Glu122, and Asp193, exist around the extracellular surface of *p*pR (Figure 1). The

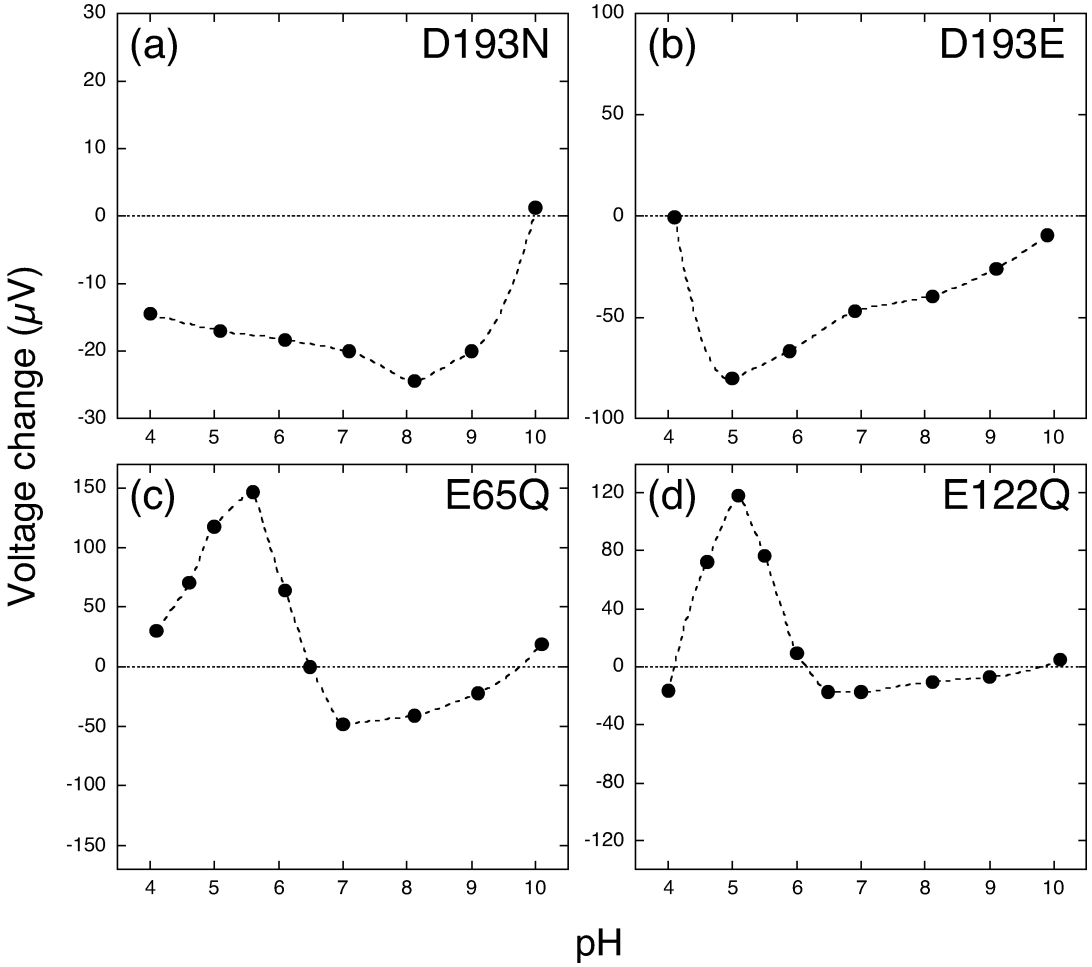

FIGURE 4: pH change of the electrode surface 10 ms after photoexcitation of the extracellular Asp or Glu mutant of *p*pR under varying pHs. The electrolyte solution contained 400 mM NaCl. Asp193 in *p*pR corresponds to Glu204 in BR, which is thought to be a component of the PRG.

corresponding residue to Glu204 in BR is conserved as Asp193 in *p*pR while that to Glu194 in BR is replaced by Pro183 in *p*pR (*26*). Site-directed mutagenesis and pH variation analysis were performed to identify the PRG in *p*pR. Light-induced pH changes at the SnO_2 electrode surface, on which PC-reconstituted *p*pR or its mutants (E65Q, E122Q, D193N, and D193E) were adhered to, were measured under varying pH. The voltage changes at 10 ms after photoexcitation that represent pH changes induced during the *p*pR-to-*p*pR_M transition are plotted against the pH of the electrolyte (Figures 3 and 4). The data show that the mutation of Asp193 converts the pH profile of the proton release. In the case of the wild type, acidification of the media 10 ms after photoexcitation was observed at pHs between 5 and 8 in the presence of Cl^-, indicating that fast proton release before *p*pR_M decay occurred under these conditions, while it was not observed at any pH under the Cl^--free condition. E65Q and E122Q mutants also showed an almost similar pH profile of fast proton release compared to the wild type. D193N and D193E mutants exhibit no fast proton release at any pH even in the presence of Cl^-. These results suggest that Asp193 is a critical component of the PRG of *p*pR that releases a proton before *p*pR_M decay in a pH- and Cl^--dependent manner.

The kinetics of *p*pR_M formation are pH-independent (*3*), and the amount of *p*pR_M accumulation formed by photoexcitation does not greatly change under pHs between 5 and 9 (data not shown). Thus, the decrease in the amplitude of the positive signal of the wild type above pH 5.5 in Figure 3 represents the pH titration curve of Asp193 in the *p*pR ground state because protonation of Asp193 in the ground state is necessary for proton release before *p*pR_M decay. On the other hand, a decrease in the positive signal below pH 5.5 may originate from a decrease in the fraction of deprotonated Asp193 in the *p*pR_M state. This is because Asp193 has the ability to release protons only when the pH of the media is higher than the pK_a of itself. Afterward, the fast pH change of the *p*pR-to-*p*pR_M transition may be explained by the balance of proton affinity of Asp193 in the ground state and *p*pR_M state as depicted in Figure 5. According to this model, the product of these two fractions (i.e., the fractions of protonated Asp193 in the ground state and deprotonated Asp193 in the *p*pR_M state) gives the pH profile curve of fast proton release. Regression analysis for the estimation of the pK_a value of Asp193 using this model was performed, and the results are listed in Table 1. The apparent pK_a values of Asp193 in the ground state were estimated to be 6.4, 6.0, and 5.6 for the wild type, E65Q, and E122Q, respectively. These values decreased to 4.9, 4.9, and 4.5, respectively, in the *p*pR_M state.

The time course of the light-induced pH change at the SnO_2 electrode surface and the flash photolysis data are compared for D193N and D193E mutants at pH 5 (Figure 6). Different from proton uptake and release under the Cl^--

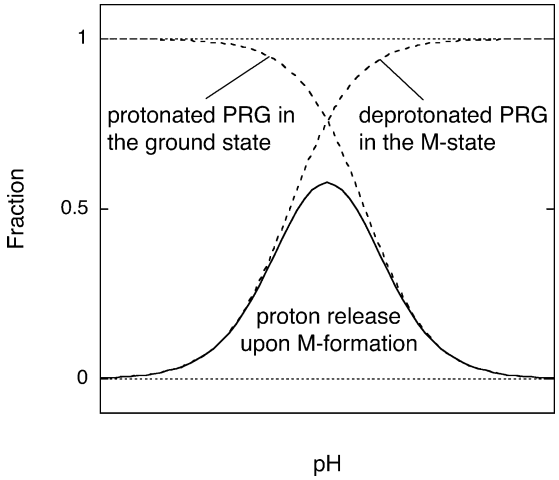

FIGURE 5: Putative relationship between the protonation state of the PRG and fast proton release before *p*pR$_M$ decay. The transient pH change might be explained by the balance of the proton affinity of the PRG between the ground state and *p*pR$_M$ state. According to this model, the product of these two fractions (i.e., protonated Asp193 in the ground state and deprotonated Asp193 in the *p*pR$_M$ state) gives the pH profile of fast proton release.

Table 1: Estimated Apparent pK_a Values of the PRG in the Ground State and M-State of Wild-Type and Mutant *p*pR[a]

	apparent pK_a value of the PRG	
	ground state	M-state
wild type	6.4	4.9
D193N	ND	ND
D193E	ND	ND
E65Q	6.0	4.9
E122Q	5.6	4.5
P183E	7.9	5.4
P183D	6.6, 9.4	5.1
complex	5.6	3.9

[a] Measurements were done in the presence of 400 mM NaCl. ND = not determined.

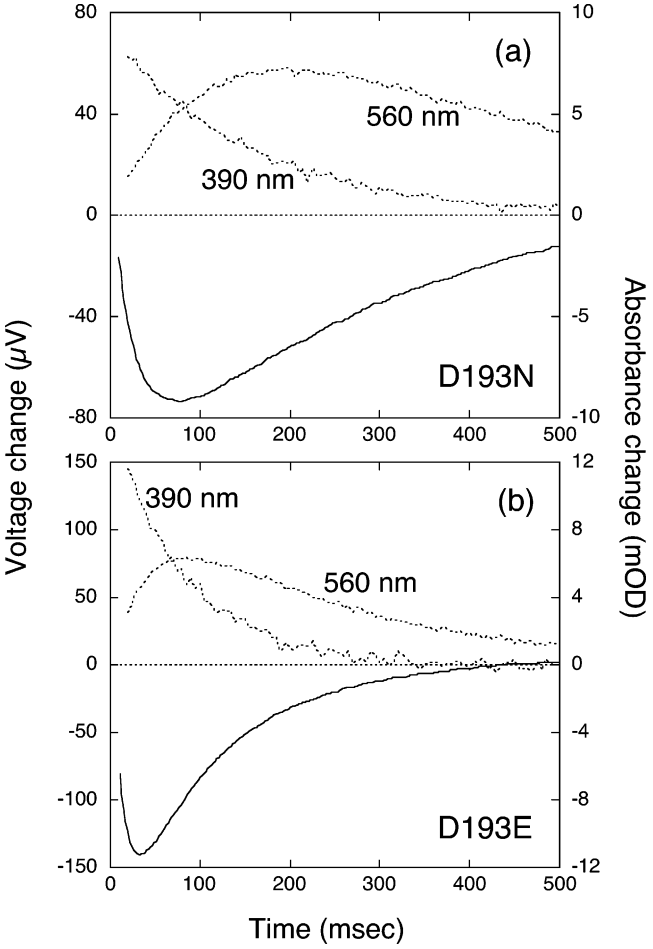

FIGURE 6: Light-induced pH and absorbance changes derived from PC-reconstituted D193N (a) and D193E (b) mutant *p*pR. The solid lines represent the light-induced pH change, and the broken lines represent the light-induced absorbance change at 390 or 560 nm. Each measurement was performed at pH 5 in the presence of 400 mM NaCl.

free condition of the wild type, those of D193 mutants did not coincide with the formation and decay of *p*pR$_O$. The proton uptake of these mutants was somewhat faster than *p*pR$_O$ formation, and a part of proton uptake is likely to begin before *p*pR$_M$ decay (*p*pR$_O$ formation). This is also confirmed by a relatively larger negative value for the voltage change before *p*pR$_M$ decay (Figure 4a,b), suggesting a perturbation of the relationship between proton uptake and release with the formation and decay of photointermediates in these mutants.

Effects of Introduction of Carboxylic Acid at Position 183 on Proton Release during the Photocycle of PC-Reconstituted ppR. Asp193 is a critical component of the PRG in *p*pR as seen from the above results. As mentioned earlier, *p*pR lacks an amino acid residue that corresponds to the PRG in BR. We introduced Asp/Glu residues instead of Pro at position 183 to produce an environment similar to that of the PRG as in BR on the extracellular surface of *p*pR. The amplitudes of the pH change for the *p*pR-to-*p*pR$_M$ transition of P183E and P183D mutants are plotted against the pH of the media in the presence or absence of Cl^- (Figure 7). It can be seen that the pH, where fast proton release before *p*pR$_M$ decay occurs, extends to a more alkaline region in these mutants than in the wild type (cf. Figure 3). The apparent pK_a values of the PRG in the ground state and the *p*pR$_M$ state in P183E were estimated to be 7.9 and 5.4 in the presence of Cl^- (Table 1). In the case of P183D, we were not able to estimate a single pK_a value for the PRG in the ground state, for reasons that are not clear at present. Instead, two pK_a values, 6.6 and 9.4, were estimated. If we assume that the pK_a value of Asp183 in P183D mutant is around 7−8, the complex pH dependence of proton release in this mutant (Figure 7) might be accounted for by considering that the pK_a in the PRG is affected by the protonation state of the 183rd amino acid. Our present results indicate that the introduction of a carboxylic residue at position 183 of *p*pR increases the apparent pK_a of the PRG. Interestingly, removing Cl^- from the solution in the cell did not affect the pK_a of the PRG in these mutants, suggesting that the negative charge of the carboxylic side chain affects Cl^- binding to the extracellular surface of *p*pR. Light-induced pH changes and absorbance changes at 390 or 560 nm were compared at pH 6 in Pro183 mutants (Figure 8). Similar to the case of the wild type, proton uptake observed after proton release during the *p*pR-to-*p*pR$_M$ transition of these mutants did not coincide with *p*pR$_M$ decay.

Effects of Transducer Binding on Proton Release during the Photocycle of PC-Reconstituted ppR. We analyzed the effects of *p*HtrII binding on proton release during the photocycle of *p*pR to consider the structure and structural

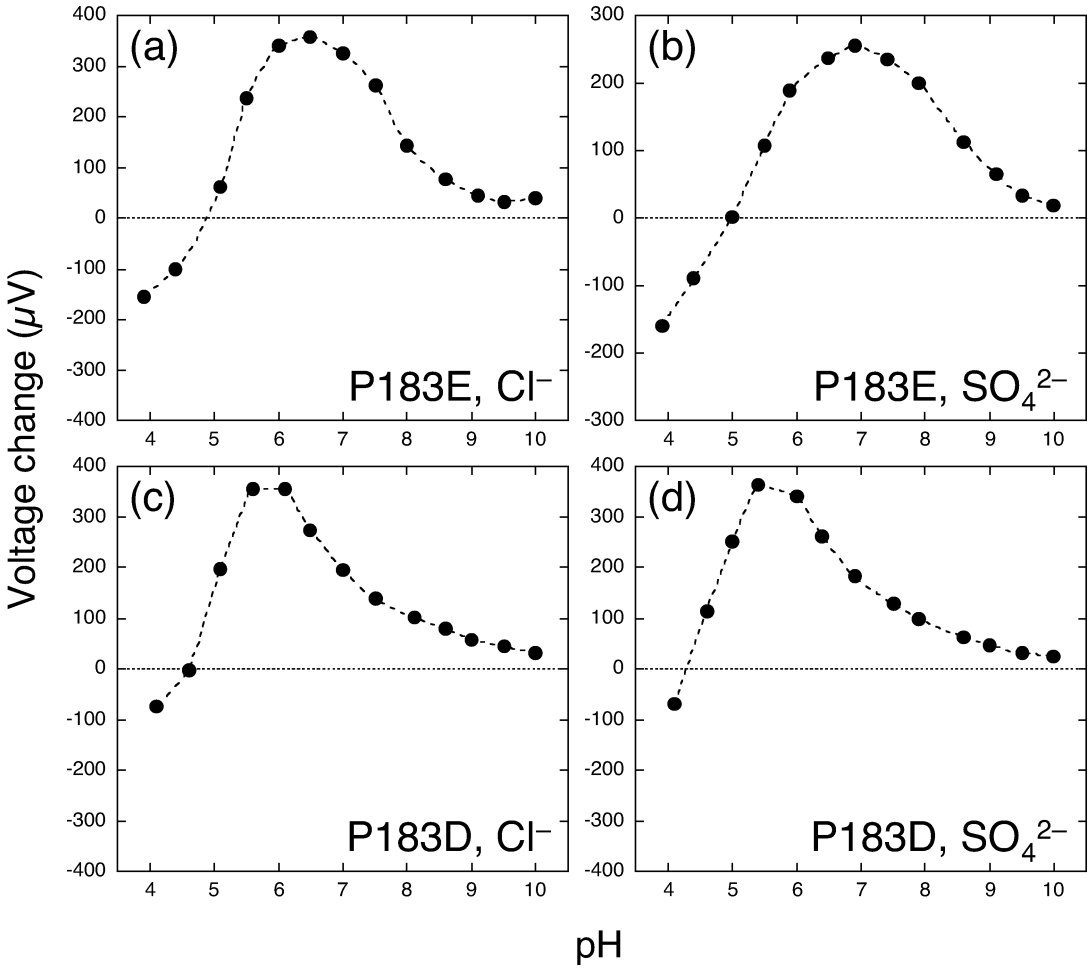

FIGURE 7: pH change of the electrode surface 10 ms after photoexcitation of the P183E (a, b) and P183D (c, d) mutant *p*pR under varying pHs. The electrolyte solution contained 400 mM NaCl (a, c) or 133 mM Na_2SO_4 (b, d). Pro183 in *p*pR corresponds to Glu194 in BR, which is thought to be a component of the PRG in BR.

changes of the complex around Asp193. A truncated *p*HtrII (*p*$HtrII_{1-159}$) (*33*) whose amino acid residues after position 159 were deleted, was used for the experiment. *p*$HtrII_{1-159}$ has sufficient ability for tight binding with *p*pR (*27*, *33*−*36*). Figure 9 shows the *p*$HtrII_{1-159}$ concentration dependency on the pH of fast proton release during the *p*pR_M formation. The molar ratios of *p*$HtrII_{1-159}$ to *p*pR are 0 (*p*pR only, closed circles), 0.5 (open circles), 1 (closed triangles), 2 (open triangles), and 3 (closed diamonds). It can be seen that the pH, at which proton release occurs before *p*pR_M decay, shifts to lower value depending upon the molar ratio of *p*$HtrII_{1-159}$ to *p*pR. These results indicate that transducer binding alters the pK_a of Asp193 in *p*pR. The pH profile curves at a higher concentration of *p*$HtrII_{1-159}$ (times two and three molar ratios) are the same, suggesting saturation of binding under these conditions because of the 1:1 (or 2:2) stoichiometry (*18*, *27*, *34*−*37*). The photocycle kinetics of the reconstituted complex samples were also measured, and a *p*$HtrII_{1-159}$ concentration-dependent decrease in the *p*pR_M decay rate (*27*) was confirmed. The *p*HtrII concentration dependence of the shifts in pK_a and *p*pR_M decay rates was similar (data not shown). The apparent pK_a value of Asp193 in the ground state and *p*pR_M state decreased to 5.6 and 3.9, respectively, under the complete binding condition (Table 1).

DISCUSSION

In the present report, the properties of proton release and uptake during the photocycle of *p*pR reconstituted with phosphatidylcholine (PC) were investigated. We showed that PC-reconstituted *p*pR releases a proton before *p*pR_M decay during the photocycle at pHs between 5 and 8 in the presence of Cl^-. These results are different from those measured in the solubilized state (*25*) or under the Cl^--free condition of the reconstituted state (*20*), where proton uptake occurs first upon *p*pR_M decay (*p*pR_O formation) followed by proton release upon *p*pR_O decay. In the case of BR, fast proton release from the proton-releasing group (PRG) to the media occurs upon BR_M formation (*38*, *39*), coinciding with primary proton transfer from the protonated Schiff base to its counterion, Asp85. The PRG in BR is thought to be Glu194 and Glu204 (*30*−*32*, *40*) or a whole hydrogen-bonded network including Arg82, Glu194, Glu204, and water molecules (*41*). When one of the Glu residues is replaced by another, BR loses the ability release protons normally, resulting in the delay of proton release until the last step of the photocycle (*30*−*32*, *40*). Our present results are interesting because PC-reconstituted *p*pR releases protons at the similar timing as BR (at least before the decay of the M-state) under certain conditions, although *p*pR lacks one of the residues corresponding to the PRG in BR.

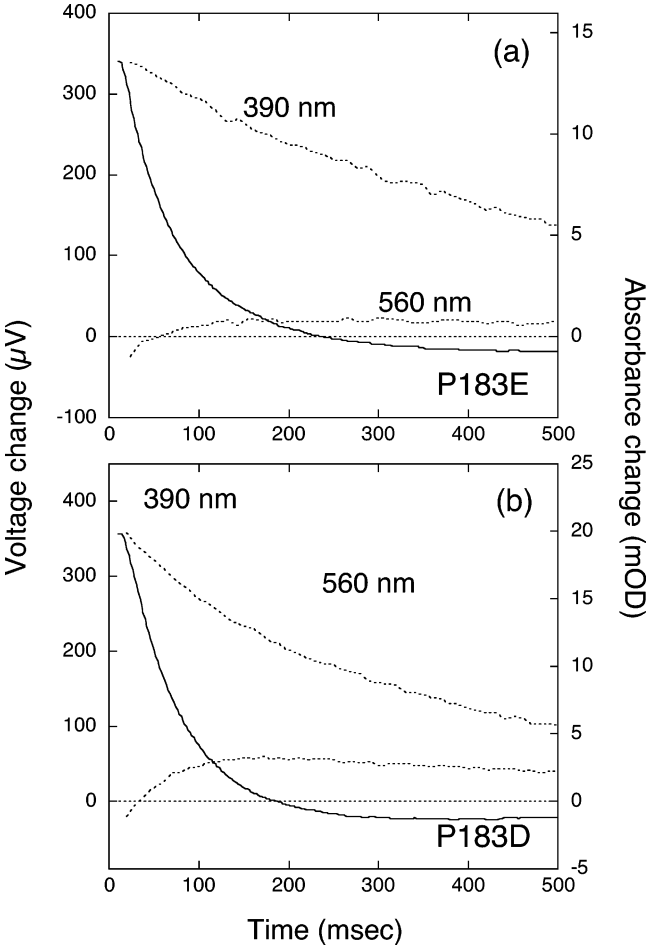

FIGURE 8: Light-induced pH and absorbance changes derived from PC-reconstituted P183E (a) and P183D (b) mutant *p*pR. The solid lines represent the light-induced pH change while the broken lines represent the light-induced absorbance change at 390 or 560 nm. Each measurement was performed at pH 6 in the presence of 400 mM NaCl.

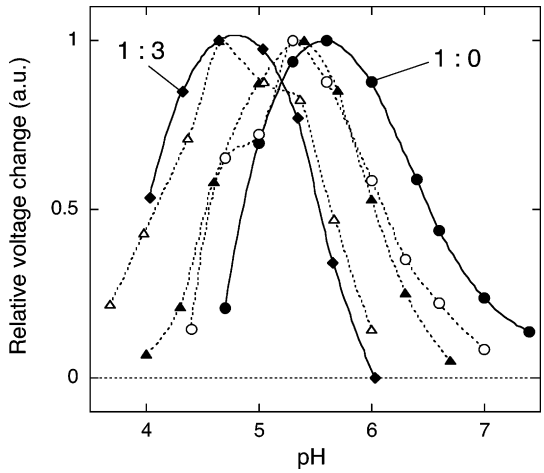

FIGURE 9: Effects of transducer binding on pH change of the electrode surface 10 ms after photoexcitation of *p*pR under varying pHs. The molar ratios of *p*HtrII to *p*pR were 0 (*p*pR only, closed circles), 0.5 (open circles), 1 (closed triangles), 2 (open triangles), and 3 (closed diamonds). The electrolyte solution contained 400 mM NaCl. The largest values for each condition were taken to be unity.

Molecular Mechanism of Proton Release during the Photocycle in ppR. From the results in Figure 4, a critical component of the PRG in *p*pR is Asp193, which corresponds

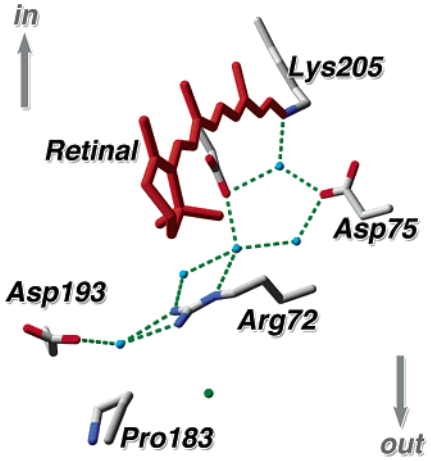

FIGURE 10: Putative hydrogen-bonding network in the extracellular channel of *p*pR. Water molecules and the putative Cl^--binding site are depicted as blue and green spheres, respectively, and putative hydrogen bonds are displayed by green broken lines. This structure was taken from the PDB (code 1H68).

to Glu204 in BR. Ikeura et al. (*Biophys. J.*, in press) estimated the pK_a of Asp193 to be 5.7 by pH titration analysis of the visible absorption spectra. The estimated value of 6.4 for the pK_a of Asp193 in the ground state in this study is not so different from 5.7, supporting each others results. Using rapid scan FTIR spectroscopy, Bergo et al. (*42*) reported the deprotonation of an unknown Asp/Glu residue whose pK_a was <7 upon *p*pR_M formation. Our present results might explain their observation (i.e., the unknown carboxylic residue is probably Asp193). Our results also reveal that the pK_a of Asp193 should decrease to 4.9 in the *p*pR_M state, implying that the environmental change occurs around Asp193 during the photocycle. This may be induced by a protein conformational change at the extracellular side similar to that of BR because the pK_a of the PRG also decreases in the M-state of BR (*46*). Thus, for *p*pR also, primary proton transfer from the protonated Schiff base to its counterion (Asp75) would lead to a similar protein conformational and environmental change around Asp193 as for BR via a hydrogen-bonding network that constitutes Arg72 and water molecules (Figure 10). In the DM-solubilized state, the pK_a of Asp193 might be lower in the ground state and/or higher in the *p*pR_M state than that in the PC-reconstituted state, which inhibits fast proton release before *p*pR_M decay. The pK_a of Asp75 of *p*pR is also likely to be affected by DM solubilization (*3*).

The present results suggest that Cl^- binding is necessary for fast proton release from Asp193 before *p*pR_M decay. In the crystal structure of *p*pR (*17*) presented by Royant et al., the existence of a Cl^--binding site was proposed between Arg72 and Asp193 (Figure 10, green sphere). Our previous study (*43*, *44*) also supports Cl^- binding around Arg72 or Asp193. Therefore, it is probable that the pK_a of Asp193 is regulated by Cl^- bound to the proposed binding site, which means that the negative charge of Cl^- electrostatically stabilizes the protonated state of Asp193 in the ground state. This may be a crucial factor for the fast proton release of *p*pR which lacks one of the corresponding residues of the PRG in BR.

The inconsistency of proton uptake, which was observed after the fast proton release upon the *p*pR-to-*p*pR_M transition,

with *p*pR$_M$ decay was revealed. The reason may be as follows: (1) There exists an unknown substate of *p*pR$_M$, which accepted the proton from the media somewhere in the protein other than the deprotonated Schiff base. Since the transition between these two *p*pR$_M$ states is spectrally silent, we might not be able to observe it from an absorbance change at 390 nm. (2) There exists two populations, one of which releases and takes in protons upon the *p*pR$_M$ formation and decay, respectively, and the other takes in and releases them upon *p*pR$_O$ formation and decay. Therefore, opposite signals may cancel each other during the *p*pR$_M$ decay or *p*pR$_O$ formation process. The origin of the inhomogeneity would be from an insufficient separation of the two pK_as of Asp193 between the ground and *p*pR$_M$ states.

Production of the BR-like PRG in ppR. Introduction of a carboxylic residue at position 183 of *p*pR increased the apparent pK_a value of the PRG from 6.4 to 7.9 (ground state) and from 4.9 to 5.4 (*p*pR$_M$ state) (Figure 7, Table 1). The pK_a value of the PRG in wild-type BR is thought to be 9.2 (*45*) and 5.8 (*46*) in the ground state and BR$_M$ state, respectively. Thus, our results imply that a more BR-like PRG, in which not only Asp193 but also Glu/Asp183 and some water molecules participate, than that of wild-type *p*pR is generated in P183E and P183D mutants. Interestingly, the Cl^- dependency of fast proton release characteristic of wild-type *p*pR disappeared in these mutants. One interpretation is as follows: a negative charge on Glu/Asp183 may inhibit Cl^- binding near the extracellular surface of *p*pR, stabilizing more strongly the protonated state of Asp193 in the ground state. The side chain of Glu/Asp183 should have a normal pK_a value and bear a negative charge above pH 5 because position 183 seems to be exposed to the media while Asp193 is located in a somewhat inner region of the protein rather than at the surface (Figure 10). It is worthwhile noting that extracellular Glu mutants in BR exhibit unusual sensitivity to Cl^- (*47*, *48*), suggesting the ability of Cl^- to substitute for the negative charge of Glu194 or Glu204.

Protein Conformational and Environmental Changes at the Extracellular Surface of ppR Induced by pHtrII Binding. In this study, the binding of the cognate transducer, *p*HtrII, lowered the pK_a of Asp193 (Figure 9). Using rapid scan FTIR spectroscopy, Bergo et al. (*42*) also suggested the effect of transducer binding on the pK_a of an unknown Asp/Glu residue, which deprotonated during the photocycle. According to the crystal structure of the *p*pR−*p*HtrII complex (*18*), binding of the transducer does not affect the structure of *p*pR, but a solid-state NMR study (*49*) detected the conformational change induced by transducer binding. Our results suggest that the conformational change occurs around Asp193, which has not been observed by X-ray crystallography. Helix F and helix G of *p*pR are thought to interact with *p*HtrII (*18*, *33*, *37*). Thus, the observation that transducer binding affects the pK_a of Asp193 is reasonable because Asp193 locates in the extracellular part of helix G. The binding of the transducer also affects the pK_a of Asp193 in the *p*pR$_M$ state. This environmental change around Asp193 in the *p*pR$_M$ state, which is induced by transducer binding, might be one of the factors responsible for signal transmission because the M-intermediate is one of the candidates for the signaling state (*50*). The differences in conformational change which occurred around Asp193 of *p*pR$_M$ between the monomer and complex should be focused on in further studies.

Concluding Remarks. The analysis of proton uptake and release of PC-reconstituted *p*pR using a SnO_2 electrode suggested the similarity between *p*pR and BR in protein conformational or environmental changes during the photocycle, at least around the extracellular channel. Thus, similar conformational changes must be used during the photocycle for the expression of different functions among archaeal rhodopsins. In the present report, conformational changes that occur before *p*pR$_M$ decay were primarily discussed. Our next focus will be on the protein conformational changes and accompanying proton transfer reactions during later steps (e.g., *p*pR$_O$) of the *p*pR photocycle. These studies will provide us with information not only about the crucial factor for signaling to the transducer but also for the functional differentiation of archaeal rhodopsins.

REFERENCES

1. Hirayama, J., Imamoto, Y., Shichida, Y., Kamo, N., Tomioka, H., and Yoshizawa, T. (1992) Photocycle of phoborhodopsin from haloalkaliphilic bacterium (*Natronobacterium pharaonis*) studied by low-temperature spectrophotometry, *Biochemistry 31*, 2093−2098.
2. Scharf, B., Pevec, B., Hess, B., and Engelhard, M. (1992) Biochemical and photochemical properties of the photophobic receptors from *Halobacterium halobium* and *Natronobacterium pharaonis*, *Eur. J. Biochem. 206*, 359−366.
3. Chizhov, I., Schmies, G., Seidel, R., Sydor, J. R., Lüttenberg, B., and Engelhard, M. (1998) The photophobic receptor from *natronobacterium pharaonis*: temperature and pH dependencies of the photocycle of sensory rhodopsin II, *Biophys. J. 75*, 999−1009.
4. Spudich, J. L., and Luecke, H. (2002) Sensory rhodopsin II: functional insights from structure, *Curr. Opin. Struct. Biol. 12*, 540−546.
5. Pebay-Peyroula, E., Royant, A., Landau, E. M., and Navarro, J. (2002) Structural basis for sensory rhodopsin function, *Biochim. Biophys. Acta 1565*, 196−205.
6. Iwamoto, M., Kandori, H., and Kamo, N. (2003) Photochemical properties of *pharaonis* phoborhodopsin (sensory rhodopsin II), *Recent Res. Dev. Chem. 1*, 15−30.
7. Oesterhelt, D., and Stoeckenius, W. (1971) Rhodopsin-like protein from the purple membrane of *Halobacterium halobium*, *Nat. New Biol. 233*, 149−152.
8. Haupts, U., Tittor, J., and Oesterhelt, D. (1999) Closing in on bacteriorhodopsin: progress in understanding the molecule, *Annu. Rev. Biophys. Biomol. Struct. 28*, 367−399.
9. Luecke, H., and Lanyi, J. K. (2003) Structural clues to the mechanism of ion pumping in bacteriorhodopsin, *Adv. Protein Chem. 63*, 111−130.
10. Matsuno-Yagi, A., and Mukohata, Y. (1977) Two possible roles of bacteriorhodopsin; a comparative study of strains of *Halobacterium halobium* differing in pigmentation, *Biochem. Biophys. Res. Commun. 78*, 237−243.
11. Varo, G. (2000) Analogies between halorhodopsin and bacteriorhodopsin, *Biochim. Biophys. Acta 1460*, 220−229.
12. Essen, L. O. (2002) Halorhodopsin: light-driven ion pumping made simple?, *Curr. Opin. Struct. Biol. 12*, 516−522.
13. Bogomolni, R. A., and Spudich, J. L. (1982) Identification of a third rhodopsin-like pigment in phototactic *Halobacterium halobium*, *Proc. Natl. Acad. Sci. U.S.A. 79*, 6250−6254.
14. Hoff, W. D., Jung, K. H., and Spudich, J. L. (1997) Molecular mechanism of photosignaling by archaeal sensory rhodopsins, *Annu. Rev. Biophys. Biomol. Struct. 26*, 223−258.
15. Shimono, K., Iwamoto, M., Sumi, M., and Kamo, N. (1997) Functional expression of *pharaonis* phoborhodopsin in *Escherichia coli*, *FEBS Lett. 420*, 54−56.
16. Luecke, H., Schobert, B., Lanyi, J. K., Spudich, E. N., and Spudich, J. L. (2001) Crystal structure of sensory rhodopsin II at 2.4 angstroms: insights into color tuning and transducer interaction, *Science 293*, 1499−1503.
17. Royant, A., Nollert, P., Edman, K., Neutze, R., Landau, E. M., Pebay-Peyroula, E., and Navarro, J. (2001) X-ray structure of sensory rhodopsin II at 2.1 Å resolution, *Proc. Natl. Acad. Sci. U.S.A. 98*, 10131−10136.

18. Gordeliy, V. I., Labahn, J., Moukhametzianov, R., Efremov, R., Granzin, J., Schlesinger, R., Buldt, G., Savopol, T., Scheidig, A. J., Klare, J. P., and Engelhard, M. (2002) Molecular basis of transmembrane signaling by sensory rhodopsin II-transducer complex, *Nature 419*, 484−487.
19. Furutani, Y., Iwamoto, M., Shimono, K., Kamo, N., and Kandori, H. (2002) FTIR spectroscopy of the M photointermediate in *pharaonis* phoborhodopsin, *Biophys. J. 83*, 3482−3489.
20. Iwamoto, M., Furutani, Y., Kamo, N., and Kandori, H. (2003) Proton-transfer reactions in the F86D and F86E mutants of *pharaonis* phoborhodopsin (sensory rhodopsin II), *Biochemistry 42*, 2790−2796.
21. Engelhard, M., Scharf, B., and Siebert, F. (1996) Protonation changes during the photocycle of sensory rhodopsin II from *Natronobacterium pharaonis*, *FEBS Lett. 395*, 195−198.
22. Schmies, G., Lüttenberg, B., Chizhov, I., Engelhard, M., Becker, A., and Bamberg, E. (2000) Sensory rhodopsin II from the haloalkaliphilic *Natronobacterium pharaonis*: light-activated proton-transfer reaction, *Biophys. J. 78*, 967−976.
23. Sudo, Y., Iwamoto, M., Shimono, K., Sumi, M., and Kamo, N. (2001) Photo-induced proton transport of *pharaonis* phoborhodopsin (sensory rhodopsin II) is ceased by association with the transducer, *Biophys. J. 80*, 916−922.
24. Schmies, G., Engelhard, M., Wood, P. G., Nagel, G., and Bamberg, E. (2001) Electrophysiological characterization of specific interactions between bacterial sensory rhodopsins and their transducers, *Proc. Natl. Acad. Sci. U.S.A. 98*, 1555−1559.
25. Iwamoto, M., Shimono, K., Sumi, M., Koyama, K., and Kamo, N. (1999) Light-induced proton uptake and release of *pharaonis* phoborhodopsin detected by a photoelectrochemical cell, *J. Phys. Chem. B 103*, 10311−10315.
26. Seidel, R., Scharf, B., Gautel, M., Kleine, K., Oesterhelt, D., and Engelhard, M. (1995) The primary structure of sensory rhodopsin II: a member of an additional retinal protein subgroup is coexpressed with its transducer, the halobacterial transducer of rhodopsin II, *Proc. Natl. Acad. Sci. U.S.A. 92*, 3036−3040.
27. Sudo, Y., Iwamoto, M., Shimono, K., and Kamo, N. (2001) *pharaonis* phoborhodopsin binds to its cognate truncated transducer even in the presence of a detergent with a 1:1 stoichiometry, *Photochem. Photobiol. 74*, 489−494.
28. Kandori, H., Shimono, K., Sudo, Y., Iwamoto, M., Shichida, Y., and Kamo, N. (2001) Structural changes of *pharaonis* phoborhodopsin upon photoisomerization of the retinal chromophore: infrared spectral comparison with bacteriorhodopsin, *Biochemistry 40*, 9238−9246.
29. Miyazaki, M., Hirayama, J., Hayakawa, M., and Kamo, N. (1992) Flash photolysis study on *pharaonis* phoborhodopsin from a haloalkaliphilic bacterium (*Natronobacterium pharaonis*), *Biochim. Biophys. Acta 1140*, 22−29.
30. Balashov, S. P., Imasheva, E. S., Ebrey, T. G., Chen, N., Menick, D. R., and Crouch, R. K. (1997) Glutamate-194 to cysteine mutation inhibits fast light-induced proton release in bacteriorhodopsin, *Biochemistry 36*, 8671−8676.
31. Dioumaev, A. K., Richter, H. T., Brown, L. S., Tanio, M., Tuzi, S., Saito, H., Kimura, Y., Needleman, R., and Lanyi, J. K. (1998) Existence of a proton-transfer chain in bacteriorhodopsin: participation of Glu-194 in the release of protons to the extracellular surface, *Biochemistry 37*, 2496−2506.
32. Essen, L. O., Siegert, R., Lehmann, W. D., and Oesterhelt, D. (1998) Lipid patches in membrane protein oligomers: crystal structure of the bacteriorhodopsin-lipid complex, *Proc. Natl. Acad. Sci. U.S.A. 95*, 11673−11678.
33. Wegener, A. A., Chizhov, I., Engelhard, M., and Steinhoff, H. J. (2000) Time-resolved detection of transient movement of helix F in spin-labeled *pharaonis* sensory rhodopsin II, *J. Mol. Biol. 301*, 881−891.
34. Sudo, Y., Iwamoto, M., Shimono, K., and Kamo, N. (2002) Association between a photointermediate of a M-lacking mutant D75N of *pharaonis* phoborhodopsin and its cognate transducer, *J. Photochem. Photobiol. B 67*, 171−176.
35. Sudo, Y., Iwamoto, M., Shimono, K., and Kamo, N. (2002) Tyr-199 and charged residues of *pharaonis* phoborhodopsin are important for the interaction with its transducer, *Biophys. J. 83*, 427−432.
36. Hippler-Mreyen, S., Klare, J. P., Wegener, A. A., Seidel, R., Herrmann, C., Schmies, G., Nagel, G., Bamberg, E., and Engelhard, M. (2003) Probing the sensory rhodopsin II binding domain of its cognate transducer by calorimetry and electrophysiology, *J. Mol. Biol. 330*, 1203−1213.
37. Wegener, A. A., Klare, J. P., Engelhard, M., and Steinhoff, H. J. (2001) Structural insights into the early steps of receptor-transducer signal transfer in archaeal phototaxis, *EMBO J. 20*, 5312−5319.
38. Drachev, L. A., Kaulen, A. D., and Skulachev, V. P. (1984) Correlation of photochemical cycle, H^+ release and uptake, and electric events in bacteriorhodopsin, *FEBS Lett. 178*, 331−335.
39. Grzesiek, S., and Dencher, N. A. (1986) Time-course and stoichiometry of light-induced proton release and uptake during the photocycle of bacteriorhodopsin, *FEBS Lett. 208*, 337−342.
40. Brown, L. S., Sasaki, J., Kandori, H., Maeda, A., Needleman, R., and Lanyi, J. K. (1995) Glutamic acid 204 is the terminal proton release group at the extracellular surface of bacteriorhodopsin, *J. Biol. Chem. 270*, 27122−27126.
41. Rammelsberg, R., Huhn, G., Lubben, M., and Gerwert, K. (1998) Bacteriorhodopsin's intramolecular proton-release pathway consists of a hydrogen-bonded network, *Biochemistry 37*, 5001−5009.
42. Bergo, V., Spudich, E. N., Spudich, J. L., and Rothschild, K. J. (2003) Conformational changes detected in a sensory rhodopsin II-transducer complex, *J. Biol. Chem. 278*, 36556−36562.
43. Iwamoto, M., Furutani, Y., Sudo, Y., Shimono, K., Kandori, H., and Kamo, N. (2002) Role of Asp193 in chromophore-protein interaction of *pharaonis* phoborhodopsin (sensory rhodopsin II), *Biophys. J. 83*, 1130−1135.
44. Ikeura, Y., Shimono, K., Iwamoto, M., Sudo, Y., and Kamo, N. (2003) Arg-72 of *pharaonis* phoborhodopsin (sensory rhodopsin II) is important for the maintenance of the protein structure in the solubilized states, *Photochem. Photobiol. 77*, 96−100.
45. Kono, M., Misra, S., and Ebrey, T. G. (1993) pH dependence of light-induced proton release by bacteriorhodopsin, *FEBS Lett. 331*, 31−34.
46. Zimanyi, L., Varo, G., Chang, M., Ni, B., Needleman, R., and Lanyi, J. K. (1992) Pathways of proton release in the bacteriorhodopsin photocycle, *Biochemistry 31*, 8535−8543.
47. Sanz, C., Lazarova, T., Sepulcre, F., Gonzalez-Moreno, R., Bourdelande, J. L., Querol, E., and Padros, E. (1999) Opening the Schiff base moiety of bacteriorhodopsin by mutation of the four extracellular Glu side chains, *FEBS Lett. 456*, 191−195.
48. Lazarova, T., Sanz, C., Sepulcre, F., Querol, E., and Padros, E. (2002) Specific effects of chloride on the photocycle of E194Q and E204Q mutants of bacteriorhodopsin as measured by FTIR spectroscopy, *Biochemistry 41*, 8176−8183.
49. Arakawa, T., Shimono, K., Yamaguchi, S., Tuzi, S., Sudo, Y., Kamo, N., and Saito, H. (2003) Dynamic structure of *pharaonis* phoborhodopsin (sensory rhodopsin II) and complex with a cognate truncated transducer as revealed by site-directed 13C solid-state NMR, *FEBS Lett. 536*, 237−240.
50. Yan, B., Takahashi, T., Johnson, R., and Spudich, J. L. (1991) Identification of signaling states of a sensory receptor by modulation of lifetimes of stimulus-induced conformations: the case of sensory rhodopsin II, *Biochemistry 30*, 10686−10692.

BI035960N